공학석사 학위논문

Graphene-FET for the Detection of DNA translocation through a Nanopore

나노포어를 통과하는 DNA의 검지를 위한 그래핀 FET 센서 연구

2014년 2월

서울대학교 대학원

재료공학부

김 지 연

Graphene-FET for the Detection of DNA translocation through a Nanopore

A DISSERTATION SUBMITTED TO

DEPARTMENT OF MATERIALS SCIENCE AND ENGINEERING

SEOUL NATIONAL UNIVERSITY

FOR THE DEGREE OF

MASTER

Jiyeon Kim

February 2014

Abstract

Nanopore is a highly promising platform for single molecule sensing and DNA sequencing. In the thesis, a new device combining nanopore structure with graphene field effect transistor (FET) is proposed as a single molecule DNA sensor. Recently, it has been reported that silicon nanowire FET fabricated on the nanopore membrane can detect local potential change arising from DNA translocation. Unlike silicon nanowire FET device, device using graphene FET can work even when ion concentrations of both chambers are identical and result in higher current change ratio. Besides, high charge carrier mobility of graphene allows fast operation of the device and higher chemical stability of graphene enables better durability in ionic solution.

A numerical model is developed to expect the device performance and to prove superiority of the device to the previously reported one. The model is verified by comparing simulation result with experimental result reported recently. The model is also used for parametric study to establish the optimum design of the device. Effect of nanopore length, nanopore diameter, graphene channel length, graphene channel width, graphene doping level, and graphene mobility are examined and analyzed. Based on the optimized design, the graphene FET nanopore device is fabricated by using conventional top down processes and associated issues are discussed.

Keywords: nanopore, graphene field effect transistor, DNA sensor

Student number: 2012-20589

TABLE OF CONTENTS

LIST OF FIGURES

Chapter 1

Chapter2

Chapter 1. Introduction

1. DNA sequencing

Deoxyribonucleic acid (DNA) is a molecule which contains genomic information of living organisms. Figure 1-1 illustrates the structure of DNA. DNA is comprised of two helical polymer strands, whose repetitive unit is called nucleotide. Each nucleotide consists of a sugar, phosphate groups and a single nucleobase. In nature, there are 4 types of nucleobases : Adenine (A), Thymine (T), Guanine (G), and Cytosine (C) and genomic information is recorded in the sequence of these nucleobases. Spacing between two adjacent nucleotides is only 0.33nm and width of single strand DNA is 1.2nm. Indeed, nature has highly integrated and miniaturized information storage system whose unit occupies only nanometric volume.

Since the discovery of structure and function of DNA, there has been great effort in reading and deciphering of this quaternary genomic code encrypted in DNA. [1] DNA sequencing not only expands our understanding on genetic phenomena occurring in living organisms but also can be applied to improve human healthcare. For example, DNA sequence at certain region can be used to estimate the risk of genetic disease or to find proper cancer treatment for each patient.

For the application of genomics to routine healthcare, it is inextricable to develop cheaper and faster DNA sequencing technology. Over the last decade, there has been great improvement of DNA sequencing methods in terms of cost and throughput (see Figure 1-2). The first DNA sequencing method, Sanger method, was developed in 1975. [4] This method employs fluorescently labeled dideoxy-nucleotides, which complementally bonds with nucleotides in DNA to be sequenced. So-called “the second generation” DNA sequencing methods have been

developed in 2000s, enabling a four orders of magnitude decrease in cost of genome sequencing. [2] However, these new methods still requires attachment of fluorescence molecules on nucleotides and duplications of DNA to amplify fluorescence signal to detectable level. These labeling and amplification processes are inevitable obstacles for further lowering of cost and increase of speed.

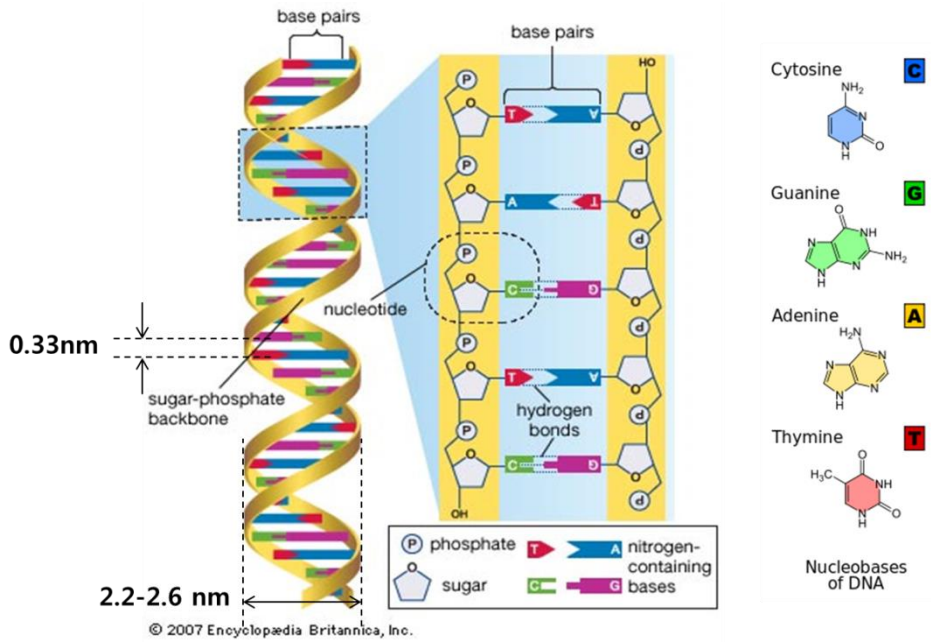

Figure 1-1 Structure of DNA [12]

(a)

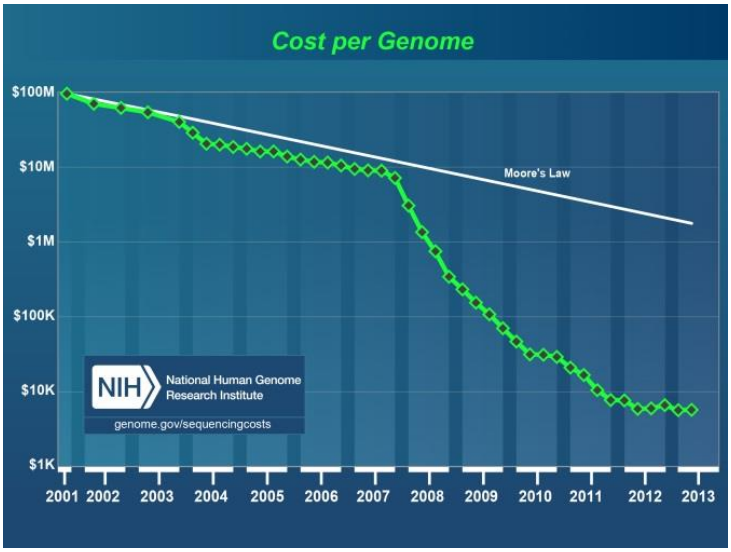

(b)

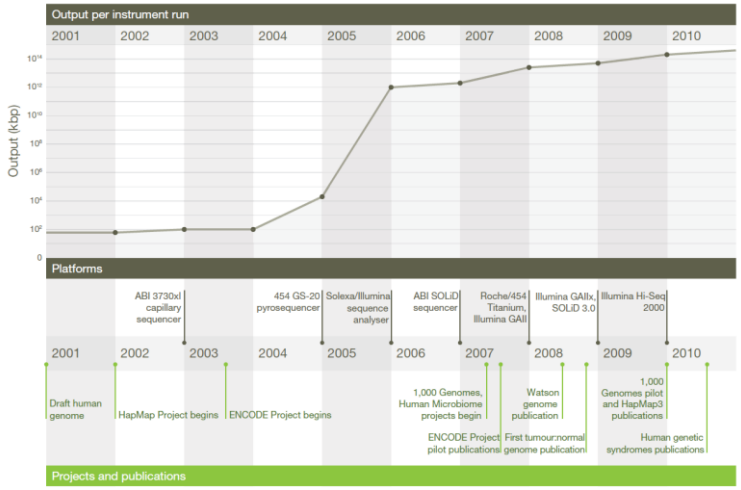

Figure 1-2 Development of DNA sequencing technology. (a) Change in the cost of sequencing a human-sized genome. [2] (b) Change in throughput of DNA sequencing methods. [3]

2. Nanopore technology

The idea of using nanopore structure for DNA sequencing was first proposed in 1989 by D. Deamer. [5] The description of the method is as follows. When a voltage is applied across an insulating membrane in which a nanometer hole is formed, DNA is electrophoretically driven to pass through the nanopore because of negatively charged phosphate backbone. Then, DNA partially blocks the nanopore and ionic current across the membrane drops depending on the volume of blocking object. Because of size difference between the four nucleobases, each A,T,G,C nucleobases produces distinct ionic current, enabling DNA sequencing. It can be noted that nanopore sequencing does not require amplification and labeling process because it relies on electrical detection of single molecule. This new type of single molecule and electrical detection based sequencing method is thought to enable cheaper and high throughput DNA sequencing.

The first experimental realization of Deamer's idea was achieved in 1996 by J. Kasianowicz, D. Deamer, and D. Branton. [6] They used a special protein, α-hemolysin, which has nanometer sized pore structure in nature. It was shown that the protein nanopore can be used to distinguish polydeoxyadnylic acid (polyA) and polydeoxycytidylic acid (polyC) single strand DNA. The experiment suggested the possibility of α-hemolysin nanopore for DNA sequencing. However, such a biological nanopore possesses limited practicality because of poor stability against environment changes such as pH, salt concentration, temperature, and mechanical stress.

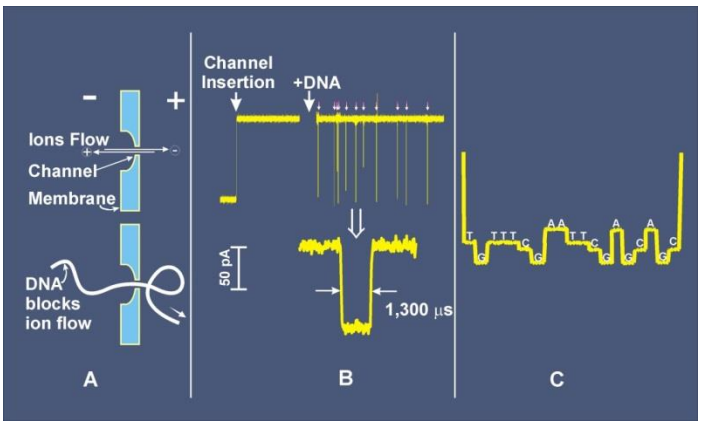

Figure 1-3 Concept of nanopore sequencing. [7] When a DNA blocks ion flow through a nanopore (part A), ionic current is decreased (part B), and each types of nucelobases results in different blockage current, enabling identification of sequence of the bases in the DNA (part C).

A solid-state nanopore, which is made of hard material, can show greater stability than biological nanopore. The typical solid-state nanopore is fabricated on silicon nitride membrane by using focused electron beam, firstly developed by C. Dekker. [8] Another advantage of solid-state nanopore over biological nanopore is controllability and modifiability. Contrary to protein nanopore with given diameter and length, dimensions of solid-state nanopore can be varied and this control of dimension is helpful for studying physics of DNA translocation and ionic transport in nanopore.

Also, in solid state nanopore, it is possible to modify original simple nanopore structure to adopt different sensing mechanisms other than ionic current method. For example, optical sensing of DNA translocation by monitoring fluorescence signal was successfully demonstrated. [9] It was also shown that fluorescence signal from multiple nanopores can be detected simultaneously, allowing highly parallel and high throughput sensing. However, this optical sensing requires complex fluorescence labeling and sample preparation step, which can be a source of errors or additional costs and time.

There are also electrical detection methods other than ionic current sensing. They read electrical current flowing in vertical to DNA translocation direction. One method is monitoring of tunneling current across the metal nanogap located on nanopore. [10] Because each nucelobase has different highest occupied molecular orbital (HOMO) and lowest occupied molecular orbital (LOMO), tunneling current across the nanogap is sensitive to the types of nucleobases in nanopore. However, the magnitude of tunneling current is too low, typically of pA, to clearly distinguish each base. Besides, fabrication of metal nanogap

aligned on nanopore is quite challenging.

Recently, Lieber group reported that silicon nanowire field effect transistor fabricated on nanopore can sensitively detect DNA passing through the nanopore. [11] When a DNA passes through a nanopore, potential around the nanopore varies, resulting in the modulation of current flow in the silicon nanowire channel. FET approach has several advantages over the other transverse current detection method. Firstly, signal to be measured is much larger(~nA) than that of tunneling current. Secondly, fabrication is much easier because electron beam can drill nanopore through both FET channel and silicon nitride membrane at a time. Furthermore, FET enables integration of a large number of FET nanopore devices on single membrane and thus, sequencing speed can be much improved.

(a)

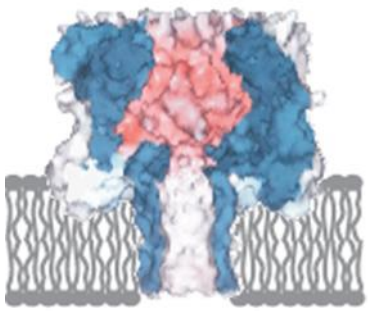

(b)

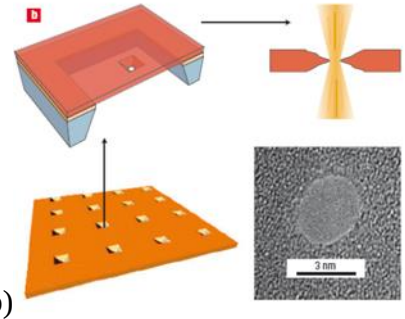

(c)

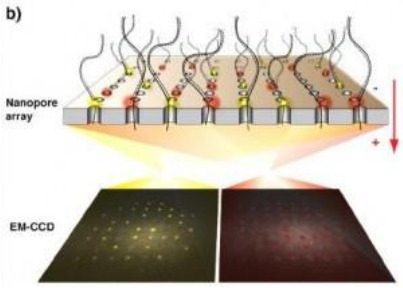

(d)

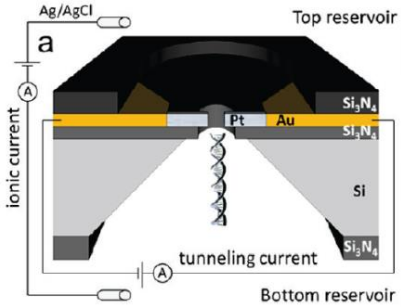

(e)

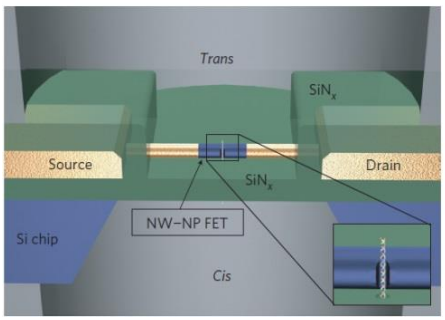

Figure 1-4 Types of nanopore sequencing platforms. (a) Protein nanopore, [6] (b) Solid state nanopore fabricated using electron beam, [8] (c) Solid state nanopore with optical detection method, [9] (d) Solid state nanopore with tunneling current detection method, [10] (e) Solid state nanopore with Field-Effect Transistor detection method. [11]

3. Outline of the dissertation

Throughout the thesis, a new nanopore device with graphene field effect transistor for the sensitive detection of DNA translocation through nanopore will be investigated.

General review on DNA structure and DNA sequencing method is presented in chapter 1. Advantages of nanopore sequencing over other DNA sequencing technologies are explained in terms of cost and throughput. Then, different nanopore platforms including FET integrated nanopore structure are introduced and advantages of FET sensing over other detection methods are discussed to justify development of the device.

In chapter 2, operation principles of FET nanopore device is explained. Based on the understanding of the device mechanism, reason for the limitation of previously developed silicon nanowire FET nanopore device is explained. Then, graphene is introduced as a solution to overcome the limitation of silicon nanowire FET nanopore device.

In the next chapter, chapter 3, numerical modeling is carried out to verify superior performance of graphene FET nanopore device compared to the silicon nanowire based device. In addition, simulation result is compared to reported experimental result and validity of the model is discussed. Lastly, parametric study is conducted to find out the optimum device parameters to be reflected on the design of the device.

In chapter 4, Device fabrication sequence is described step by step. Introduction of graphene to conventional CMOS process caused several problems and such fabrication issues are discussed in detail.

Finally, in chapter 5, overall work on graphene FET nanopore device is summarized including motivation of the development of the device, simulation results manifesting superiority of graphene based device to previously reported silicon nanowire based device, device optimization based on parametric study, validity of the numerical model and outlook of further work.

4. References

[1] E. D. Green, M. S. Guyer, National Human Genome Research Institute, *Nature* **470**, 204 (2011)

[2] http://www.genome.gov/sequencingcosts/ (12 Dec. 2013)

[3] E. R. Mardis, *Nature* **470**, 198 (2011)

[4] F. Sanger, A. R. Coulson, *J. Mol. Biol.* **94**, 441 (1975)

[5] E. Pennisi, *Science* **336**, 534 (2012)

[6] J. J. Kasianowicz, E. Brandin, D. Branton, D. W. Deamer, Proc. *Natl. Acad. Sci. U.S.A* **93**, 13770 (1996)

[7] http://www.mit.edu/~kardar/research/seminars/translocation /Introduction.html (12 Dec. 2013)

[8] A. J. Storm, J. H. Chen, X. S. Ling, H. W. Zandbergen, C. Dekker, *Nature Mater.* **2**, 537 (2003)

[9] B. McNally, A. Singer, Z. Yu, Y. Sun, Z. Weng, A. Meller, *Nano Lett.* **10**, 2237 (2010)

[10] A. P. Ivanov, E. Instuli, C. M. McGilvery, G. Baldwin, D. W. McComb, T. Albercht, J. B. Edel, *Nano Lett.* **11**, 279 (2011)

[11] P. Xie, Q. Xiong, Y. Fang, Q. Qing, C. Lieber, *Nature Nanotech.* **7**, 119 (2012)

[12] (12 Dec. 2013) http://www.britannica.com/EBchecked/media/106485/

http://commons.wikimedia.org/wiki/File:Difference_DNA_RNA-EN.svg

Chapter 2. Graphene FET for the detection of DNA translocation through a nanopore

1. Introduction

In this chapter, operation principles of FET nanopore device are described in order to explain reasons for the limitation of previously reported silicon nanowire FET nanopore. Then, reason why graphene can solve the problem is discussed and development of graphene FET nanopore device is justified.

2. Operation principles

FET detection mechanism in nanopore, which is described below was firstly developed by Xie et al. [1] Their explanation is as follows.

When a potential is applied between Ag/AgCl electrodes across the nanopore membrane, potential drop between these two electrodes comprises of three parts. The First one is potential drop across the trans chamber (V_T). The second part is potential drop in nanopore, which is typically the largest portion (V_P). The remaining part is potential crop across the cis chamber (V_C). The potential distribution when transmembrane voltage is applied is presented in Figure 2-1 (a) and (b). If we assume that FET is fabricated on the nanopore membrane, FET monitors potential at its location by changing drain current as a function of local potential. The equivalent circuit model for the FET nanopore system is depicted in Figure 2-1 (c). There are three resistance components representing resistance of trans chamber, nanopore, and cis chamber, respectively. Note that gate potential applied to FET corresponds to potential drop across the trans chamber (V_T), which says that FET detects local potential at the boundary between nanopore and trans chamber.

When DNA exists inside the nanopore, pore resistance increases because DNA blocks the movement of ions, leading to increase in potential drop across the nanopore (V_p). This means that potential at the interface between trans chamber and nanopore, where FET is located, is changed. The change of the potential (ΔV) is detected by FET by change of drain current. The amount of drain current change is determined by a FET device characteristic which is dependence of drain current as a function of gate voltage.

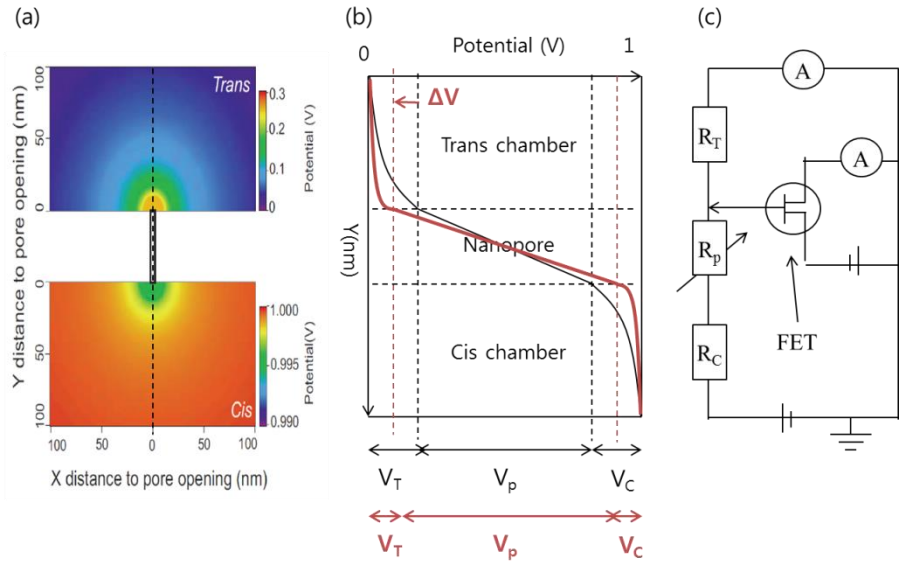

Figure 2-1 Detection mechanism of FET nanopore device. (a) Potential distribution in cis and trans chamber. [1] (b) Potential along the axis of nanopore (X=0). The black line represents an example of potential without DNA. When DNA exists in the nanopore, potential drop across the nanopore increases as indicated in the red line. (c) Equivalent circuit model of FET nanopore device.

3. Limitation of silicon nanowire FET nanopore

The previously reported FET nanopore device made use of silicon nanowire as a channel material. [1] Although the silicon nanowire FET nanopore system was shown to successfully detect DNA translocation events, there were two limitations in the experimental results. (see Figure 2-2) One problem was that detection was not possible when KCl concentrations of both cis and chamber were 1M, which is the most typical condition in nanopore studies. The other was that relative amount of FET current change to initial FET current, $\Delta IFET/IFET=0.4\%$, was too small to sensitively detect DNA translocation events.

The origin of these problems lies in the FET device characteristic which is dependence of drain current as a function of gate voltage. Figure 2-3 illustrates typical gate voltage – drain current curve of typical p-type silicon nanowire FET. It can be seen that there is minimum gate voltage required to flow drain current, which is called threshold voltage. The threshold voltage depends on the doping concentration of the nanowire. Nevertheless, current cannot flow around 0 voltage.

The problem arises at this point. In typical 1M buffer KCl concentration, the portion of the potential drop throughout the nanopore is much larger than other two parts. Hence, FET operates at very small gate voltage close to 0V. Therefore, silicon nanowire cannot effectively work at the 1M/1M concentration condition. In contrast, when KCl concentration of trans chamber is decrease to 10mM while concentration of cis chamber is remained as 1M, the relative resistance of trans chamber increases and the portion of potential drop in trans

chamber is not negligible anymore. Thus, it was able to detect DNA translocation in the gradient ion concentration condition.

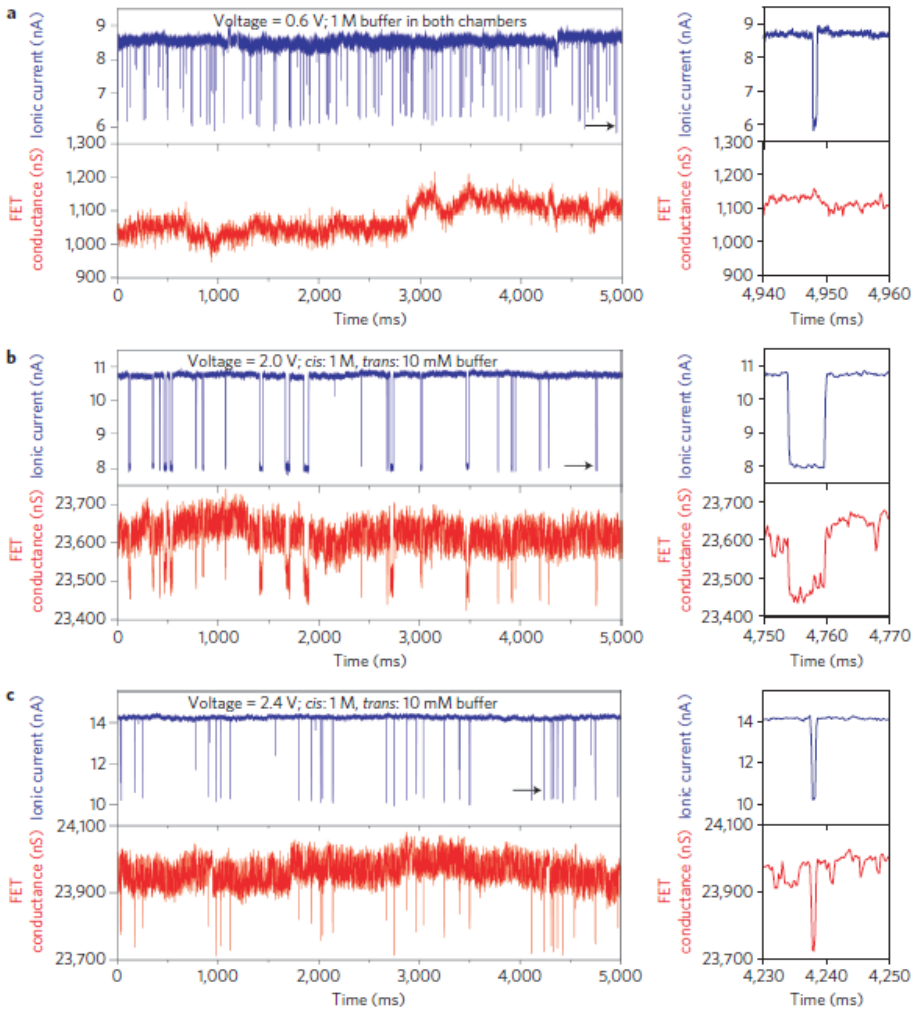

Figure 2-2 Experimental results on the detection of DNA translocation using silicon nanowire FET nanopore. [1] (a) Simultaneously recorded ionic current and FET conductance signals with both chambers filled with 1M KCl buffer, voltage 0.6V and 6nM pUC 19 dsDNA in the cis chamber. (b) Voltage 2V, trans chamber KCl buffer concentration of 10mM, cis chamber KCl buffer concentration of 1M. (c) Voltage 2.4V with the same KCl concentration with (b).

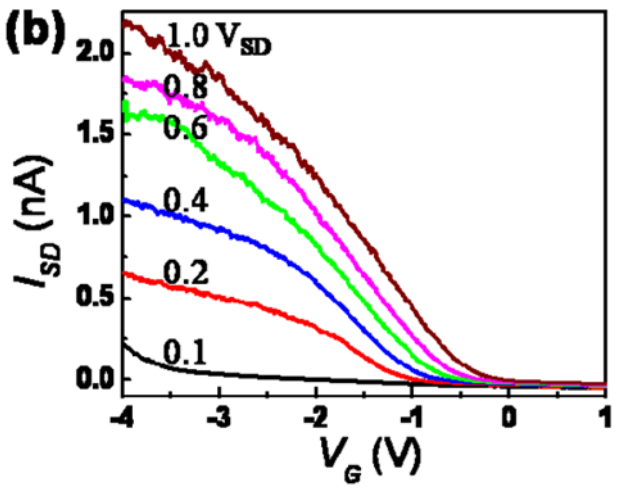

Figure 2-3 Gate voltage – drain current curve of a p-type silicon nanowire FET. [2]

4. Graphene FET nanopore

Graphene is one atom thick 2D sheet of hexagonally arranged carbon atoms. Figure 2-4 shows electronic band structure of graphene. Cone shaped valence band and conduction band touches at a point, called Dirac point. When a negative gate voltage is applied to lower the Fermi level below the Dirac point, holes are accumulated in graphene and graphene channel conductivity increases. On the other hand, when a positive voltage is applied to make Fermi level lie upper the Dirac point, electrons are accumulate and graphene channel conductivity increases again. Therefore, graphene has v shape drain current as a function of gate voltage as described in Figure 2-4. The conductance minimum corresponds to when Fermi level lies exactly on the Dirac point.

Unlike silicon, graphene FET sensor can effectively work at 0V because drain current still changes near zero gate voltage. Therefore, it is be expected that graphene FET is possible to detect DNA translocation even in 1M KCl concentration condition. Thus, graphene FET nanopore device has wider operation condition window.

Also, it is well known that graphene has excellent mobility compared to other FET materials including silicon as summarized in Figure 2-6. The high mobility of graphene allows fast operation of the sensor. Additionally, graphene is advantageous due to better stability in ionic solution [5] and possibility of top down fabrication, which makes fabrication of the device more controllable.

To summarize, it can be concluded that graphene FET nanopore sensor is expected to be advantageous in aspects of working salt concentration, operation speed, stability in ionic salutation and

facileness of fabrication. In the next chapter, numerical simulation is conducted to further verify that graphene FET nanopore device can overcome the two limitations of the silicon nanowire device.

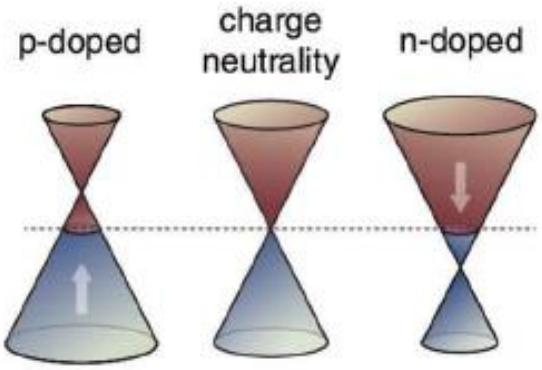

Figure 2-4 Schematic of band structure shift as gate voltage dopes graphene above and below the Dirac point. [3]

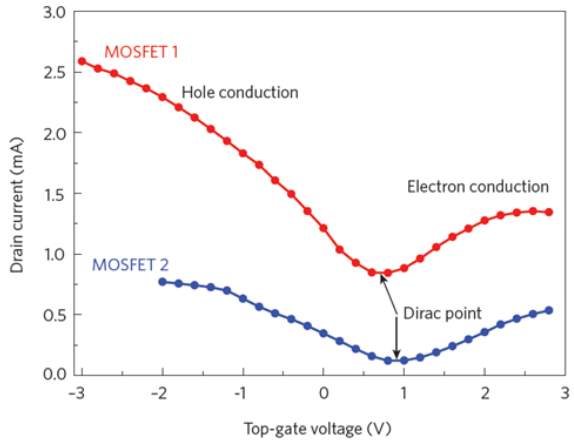

Figure 2-5 Typical transfer characteristics for two MOSFETs with large-area-graphene channels. [4]

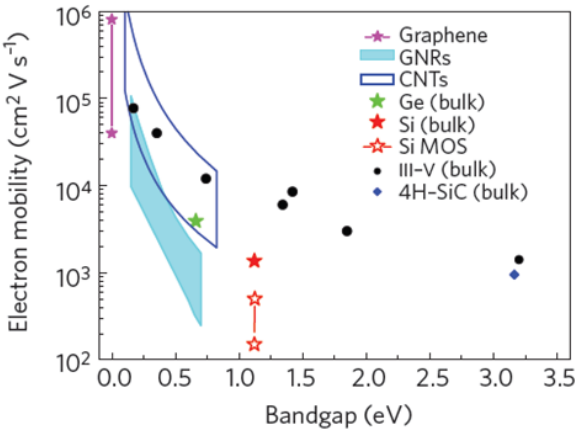

Figure 2-6 Electron mobility versus bandgap in low electric fields for different materials. [4]

5. References

[1] P. Xie, Q. Xiong, Y. Fang, Q. Qing, C. Lieber, *Nature Nanotech.* **7**, 119 (2012)

[2] S. H. Lee, K. J. Jeon, W. Lee, A. Choi, H. Jung, C. Kim, M. Jo, *J. Korean Phy. Soc*. **55**, 232 (2009)

[3] N. O. Weiss, H. Zhou, L. Liao, Y. Liu, S. Jiang, Y. Huang, X. Duan, *Adv. Mater.* **24**, 5782 (2012)

[4] F. Schwierz, *Nature Nanotech.* **5**, 487 (2010)

[5] C. Schmidt, *Nature* **483**, S37 (2012)

Chapter 3.

Numerical Modeling of graphene FET-nanopore

1. Introduction

In this chapter, numerical modeling of the graphene FET nanopore is introduced to test whether this new system can overcome the two limitation of silicon nanowire FET nanopore device. One is the limited detection of DNA when ion concentrations of both cis and trans chamber are 1M. The other problem is too low signal change relative to original current level. Then, simulation result is compared to experimental result recently reported by F. Traversi et al. [1] Lastly, parametric study is carried out to find the optimum device design.

2. Numerical modeling method

A commercial Finite Element Method simulation tool (COMSOL multiphysics 4.2) was used for the numerical modeling. COMSOL has advantage in solving combination of several correlated governing equations like our problem. The overall simulation is comprised of two subparts. In the first step, potential distribution throughout the entire nanopore system is solved and in the next step, current flowing in graphene channel is calculated from the potential distribution data. (see Figure 3-1)

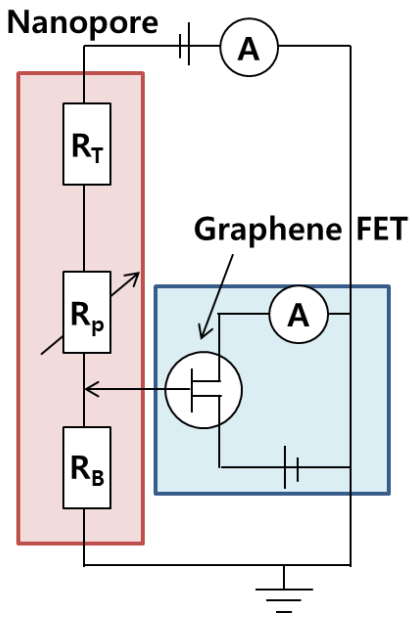

Figure 3-1 Model structure for graphene FET nanopore device. The model comprises of two parts: nanopore model and graphene FET model.

(a)

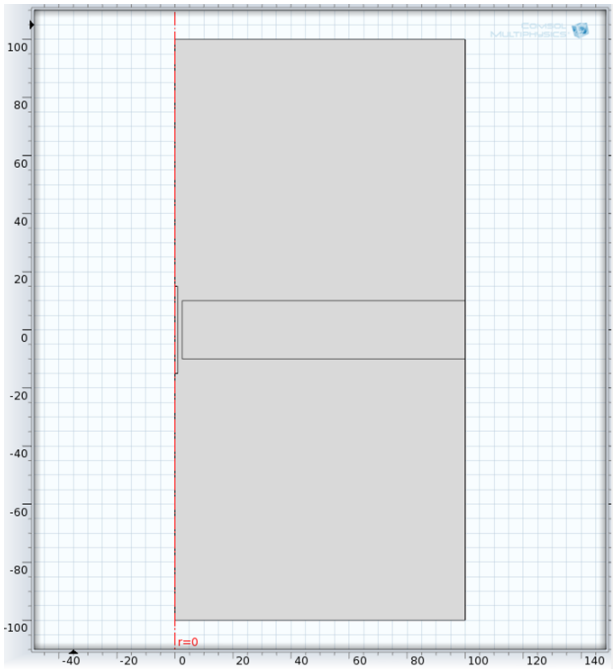

(b)

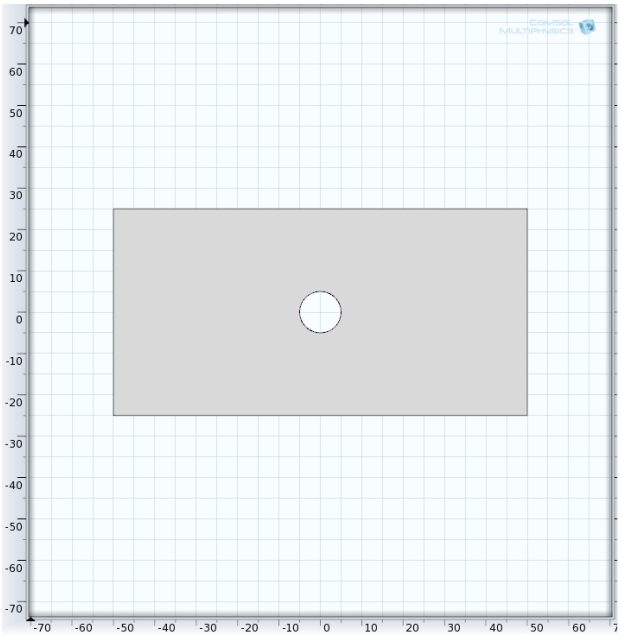

Figure 3-2 Model geometry for (a) nanopore simulation, (b) graphene FET simulation.

In the first part, following two differential equations are solved to solve electric potential V and two ion concentrations c_K, and c_{Cl}.

- Poisson equation

$$-\varepsilon_0 \varepsilon_r \nabla^2 V = \sum_{i=1}^{n} F z_i c_i$$

- Nernst-Plank equation

$$\nabla \cdot N_i = \nabla \cdot (-D_i \nabla c_i - z_i e \mu_i c_i \nabla V) = 0$$

Where ε_r is the relative permittivity of water, F is the Faraday constant, zi is the valence of each ion, D_i is the diffusion coefficient of each ion, μ_i is the mobility of each ion, N_i is the flux of each ion.

Axis symmetry was used to simplify 3D problem to 2D problem in r-z plane. The model geometry used for simulation is shown in Figure 3-2. The large rectangle in the middle of simulation domain represents membrane with thickness of 20nm and there is a nanopore with radius of 2.5nm. DNA is modeled as a rod structure with radius of 1nm and length of 30nm. The potential and concentration of ions are solved in the electrolyte region. Boundary condition imposed at each boundaries is as follows.

- Application of potential : V=0 at z=-100nm boundary, V=-200mV at z=100nm boundary

- No surface charge : at all boundaries except z=-100nm, z=100nm boundaries.

$$\vec{n} \cdot (-\varepsilon_0 \varepsilon_r \nabla V) = 0$$

- Concentration restriction : both ion concentrations are relaxed toward the bulk salt concentration 1M, C_K=C_{Cl}=1M, at boundaries far from the pore, z=+100nm, z=-100nm, and r=100nm boundaries.

- Membrane and DNA is impermeable to ions at all boundaries on membrane and DNA.

$$\vec{n} \cdot \overrightarrow{N_i} = 0$$

Note that in our model, surface charge of membrane is neglected because ion concentration of 1M is high enough to screen the surface charge within subnanometer.

Ionic current can be calculated by integrating the resulting ionic fluxes.

$$I_{ion} = \sum z_i F N_i$$

In the second part, where graphene FET is modeled, conductivity of graphene channel at each position is calculated from the potential value calculated from the first step of simulation. The conductivity and electric potential has the following relationship.

$$\sigma = \frac{\beta_G}{2} e^3 \mu (V + V_i\ )^2$$

Where, βG is a constant with value of $1.5 \times 10^{14} eV^{-2} cm^{-2}$, e is elementary charge of electron, μ is electron or hole mobility, V is applied electrical potential, and Vi is potential corresponding to initial

doping of graphene due to substrate or chemical residues on graphene. In the simulation, $\mu=10^4 cm^2/Vs$ and $V_i=20mV$ were used as default values. Potential under the membrane $V(r,z=-L_{pore}/2)$ is coupled to the second model to calculate potential at each (x, y) coordinates, V(x,y). Then, conductivity $\sigma(x,y)$ is easily calculated from the above equation. Then, source drain bias of 20mV is applied across the graphene channel. In the next step, Ohm's law is used to calculate flux of charge carriers, J.

$$J = \sigma E_{ll}$$

Finally, FET drain current is calculated by integrating flux.

$$I_{FET} = \int J_x dy$$

3. Numerical modeling results

The translocation of DNA was simulated by changing z position of DNA, Z_{DNA}. The membrane is located at z=0. The simulation result is presented in Figure 3-3. It can be seen that when DNA passes through the nanopore, ionic current drops and FET current increases. The increase in FET current can be explained by examining potential curve along the r=0 line. (See Figure 3-4.) When a DNA passes through the nanopore, resistance of the nanopore increases and relative portion of the potential drop occurring in nanopore also increases. Then, potential at the graphene channel (z=-10nm) increases in the amount of 1.33mV. Because graphene is set to be n-type (Vi=20mV, positive sign means n-type), positive change of potential results in increase in the number of electrons in graphene, leading to increase in FET current.

Note that graphene FET device can work when ion concentrations of both chambers are 1M, which was not possible by using silicon nanowire FET device. Also, ratio of FET current change to initial FET current is 1.86%, which is much larger than that of silicon nanowire FET device. [2]

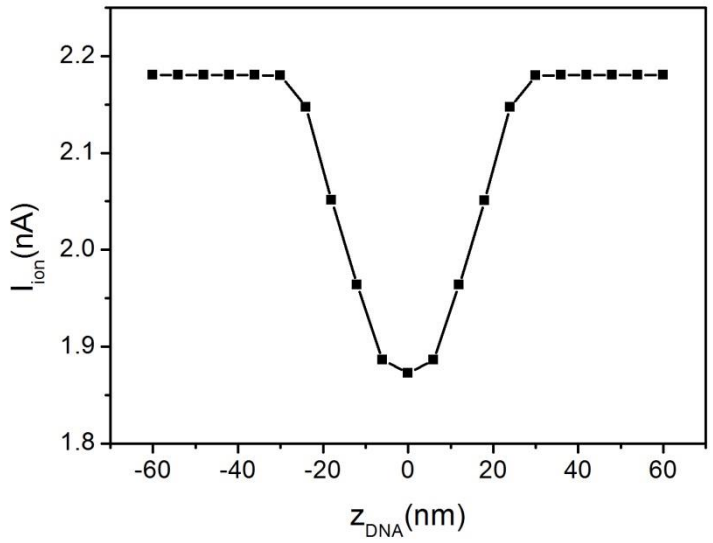

(a)

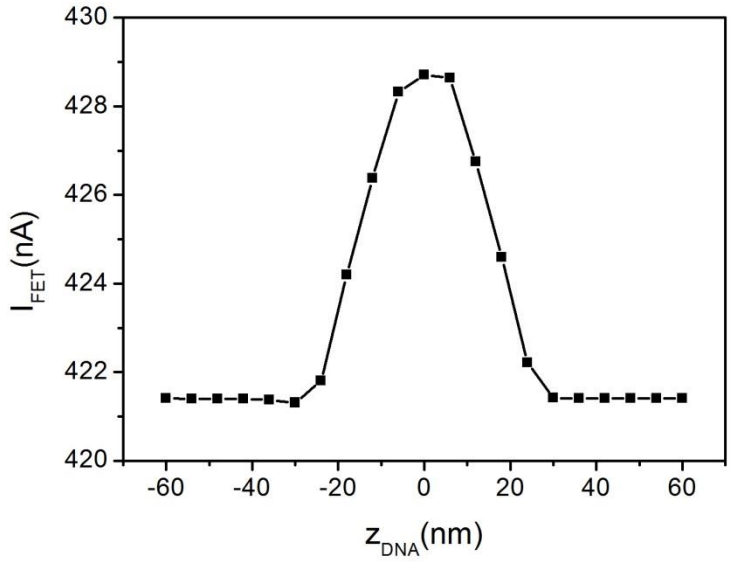

(b)

Figure 3-3 Simulation result of (a) ionic current as a function of DNA position, (b) FET current as a function of DNA position.

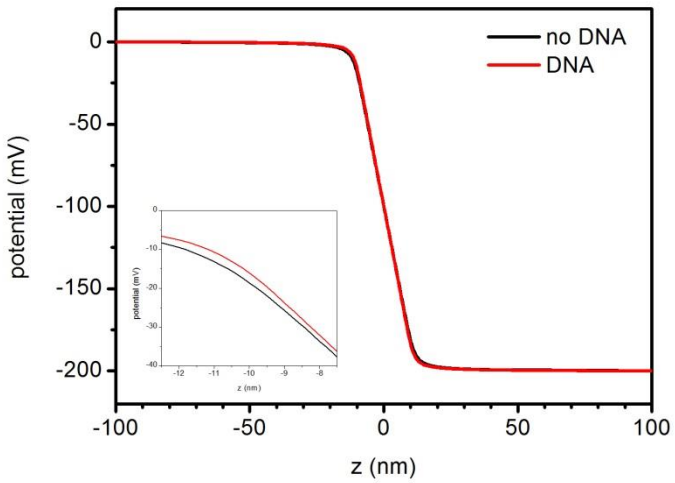

Figure 3-4 Potential calculation result along the r=0 line. When DNA blocks the nanopore (red line), small increase of potential of 1.33mV is resulted at z=-10nm position, where graphene channel is located.

4. Comparison with experimental results

Recently, F. Traversi et al. reported successful detection of DNA using graphene FET nanopore device. Comparison between simulation result and the experimental result can be done to verify the validity of the numerical model. Figure 3-10 shows simultaneous ionic current and FET current during translocations of pNEB DNA in 10mM KCl. It was possible to find the values of the device parameters for simulation. The simulation results showed right sign of signal change and the order of signal. However, simulation result showed smaller $\Delta I_{FET}/I_{FET}$ (4.4%) than that of measured value (11%). This two time smaller signal cannot be reasonably explained by small deviation of device parameter. According to their explanation, it seems that surface charge of the nanopore seems to play significant role. Further improvement of the model developed in this thesis can be achieved by inclusion of surface charge effect.

(a)

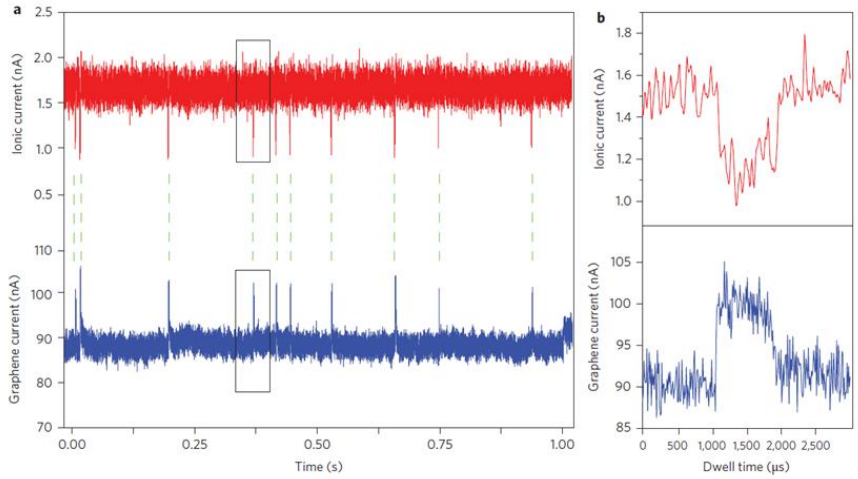

Figure 3-5 Simultaneous detection of DNA translocations in ionic and graphene current. [1]

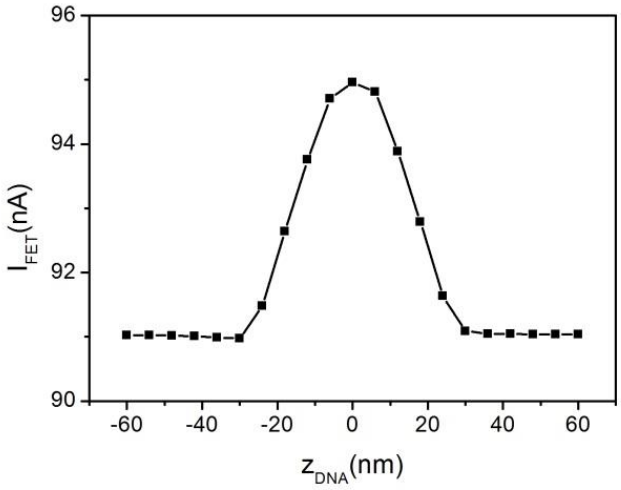

Figure 3-6 Simulated FET current as a function of DNA position. (ion concentration=10mM, d_{pore}=10nm L_{pore}=20nm, w=200nm, L=100nm, Vi=10mV μ=2700cm^2/Vs $d_{plasmid}$=2nm, V_{trans}=200mV, V_{SD}=20mV)

5. Optimization of device parameter

In the simulation developed above, there are several device parameters that can affect the performance of the device. These parameters are pore length, pore diameter, graphene channel length, graphene channel width, electron mobility, and initial doping of graphene. In the followings, effects of such parameters on the sensitivity of the device, which are represented by the values of $\Delta I_{FET}/I_{FET}$, to figure out optimum device design.

5.1 Effect of pore geometry

$\Delta I_{FET}/I_{FET}$ was calculated for different pore diameters and pore lengths. Figure 3-7 shows that smaller pore diameter and smaller pore length results in higher $\Delta I_{FET}/I_{FET}$. This can be interpreted by a simple analytical model.

Gate potential applied to graphene FET, V_B can be expressed as

$$V_B = \frac{R_B}{R_T + R_P + R_B} V$$

Where RB and RT is resistance associated with bottom and top chamber, respectively, Rp is pore resistance, V is potential applied between two Ag/AgCl electrodes.

Gate potential change due to presence of DNA can be written as

$$\Delta V_B = \frac{-R_B}{(R_T + R_P + R_B)^2} V \Delta R_p$$

Each component can be expressed as a function of resistivity of ions ρ, pore diameter d, pore length L, blocking area of DNA ΔA.

$$R_T = R_B = \frac{\rho}{2d}$$

$$R_P = \frac{4\rho L}{\pi d^2}$$

$$\Delta R_p = -\frac{16\rho L}{(\pi d^2)^2}\Delta A$$

By inserting the above three equations into ΔV_B equation results in

$$\Delta V_B = \frac{V\Delta A}{2dL\left(1+\frac{\pi d}{4L}\right)^2}$$

Therefore, gate potential change due to DNA translocation is large when pore diameter is small. Also, according to the equation ΔV_B has maximum when L=πd/4. For the pore diameter of 5nm, maximum gate potential change is achieved when the length of the pore is 3.9nm. Therefore, shorter pore length is desirable to get high sensitivity of the device. In order to reduce pore length, it is important to thickness of the membrane. Conventional LPCVD grown SiN membrane cannot be made thinner than 20nm. Hence, instead of drilling nanopore on SiN membrane, patterned SiN membrane is used to fabricate graphene FET on top of it and then Al_2O_3 layer is deposited by ALD, on which nanopore is drilled subsequently. By this way, it is possible to fabricate nanopore with length of less than 10nm.

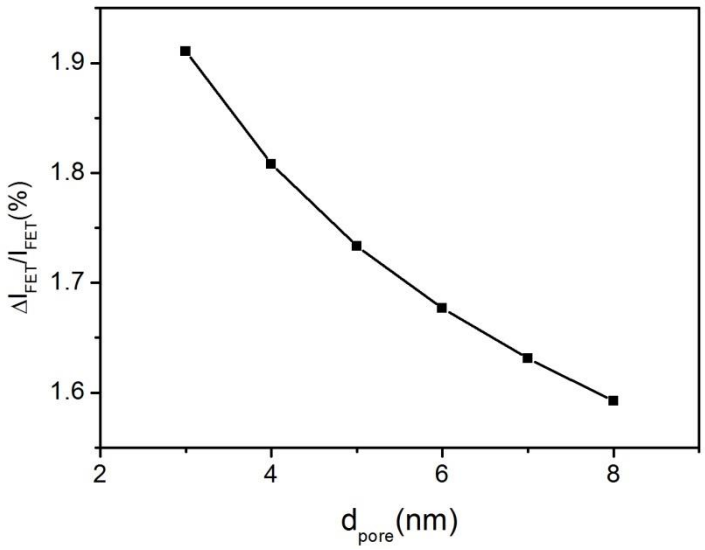

(a)

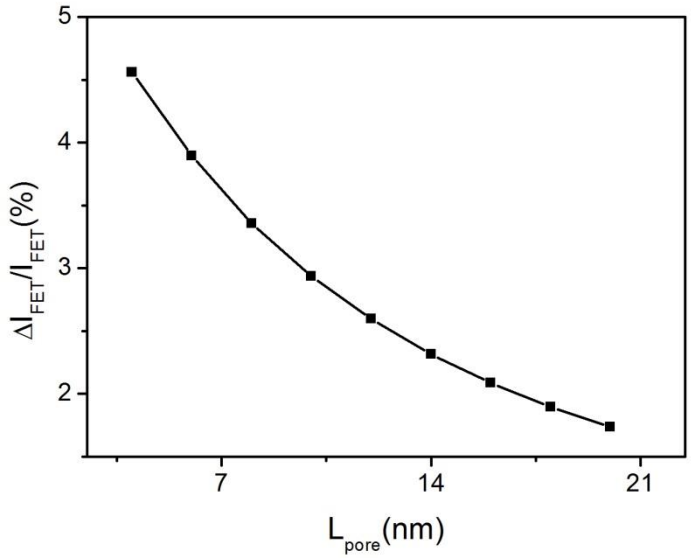

(b)

Figure 3-7 Effect of (a) pore diameter, (b) pore length on the relative change of FET current.

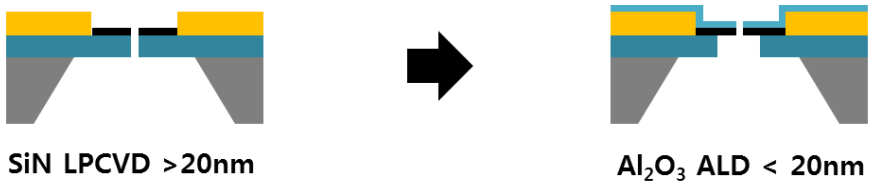

Figure 3-8 Schematics of graphene FET nanopore device in which nanopore is drilled on (a) SiN layer, (b) Al_2O_3 layer. The second design is preferable to form shorter pore length.

5.2 Effect of graphene channel geometry

Dependences of $\Delta I_{FET}/I_{FET}$ on channel length and width are depicted in Figure 3-9. Clearly, shorter and narrower graphene channel gives rise to higher relative signal change. This is because only small area around the nanopore undergoes change during DNA passage. Hence, the smaller the graphene channel, the larger portion of responding area. It leads to higher sensitivity of the device.

However, shorter and narrower graphene can be severely damaged while imaging in TEM. Recently, M. Puster et al. reported that the e-bema induced damage can be minimized by operating in STEM mode. [3]

5.3 Effect of graphene quality

In next step, effect of graphene quality is examined. Dependence on initial doping potential, Vi suggests that small doping results in larger $\Delta I_{FET}/I_{FET}$. (See Figure 3-10.) However, the absolute value of ΔI_{FET} also becomes zero when Vi approaches to 0. Also, it is not easy to control Vi value beccuase it depends on many factors such as types of substrate, chemical residues on graphene, thermal treatment.

Mobililty of graphene does not affect the relative change of FET current, $\Delta I_{FET}/I_{FET}$. (See Figure 3-11.) This is because both ΔI_{FET} and I_{FET} are proportional to the mobility. Instead, the absolute value of ΔI_{FET} increases when the mobility is high. Hence, fabrication of high mobility graphene is desirable.

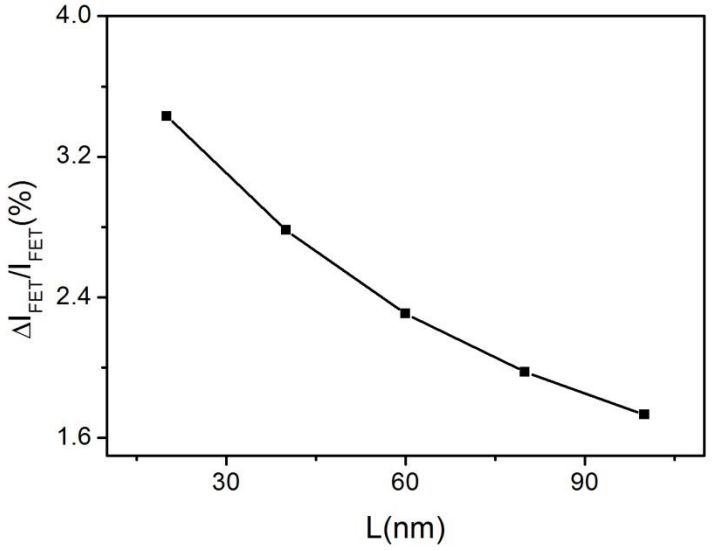

(a)

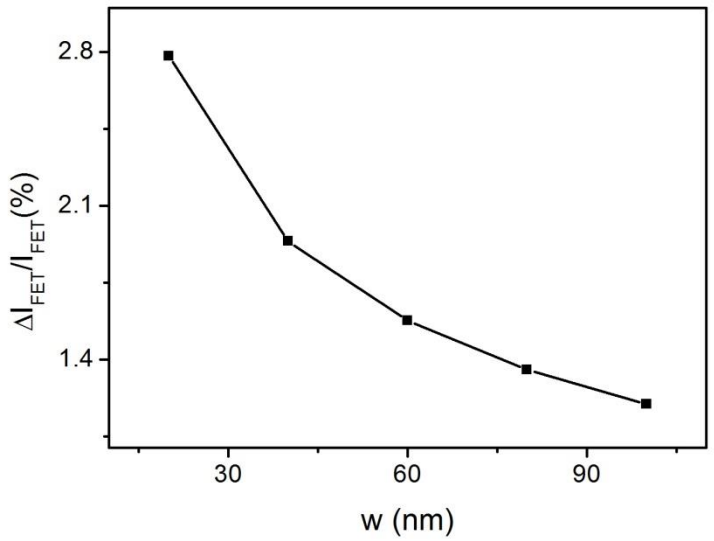

(b)

Figure 3-9 Effect of (a) graphene channel length, (b) graphene channel width on the relative change of FET current.

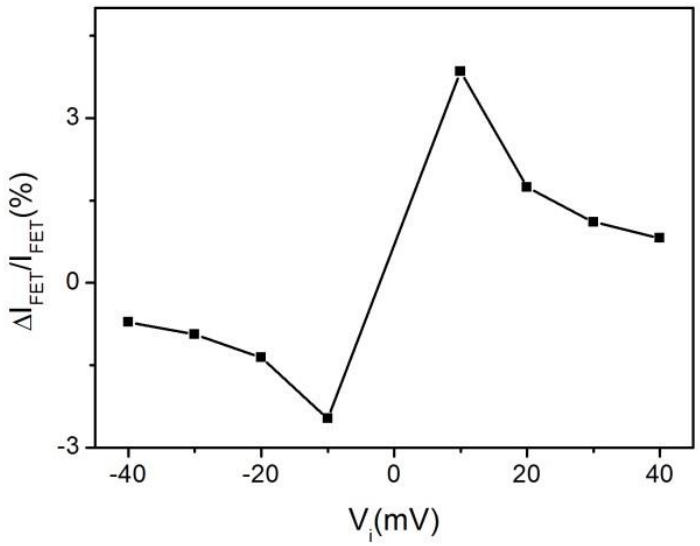

(a)

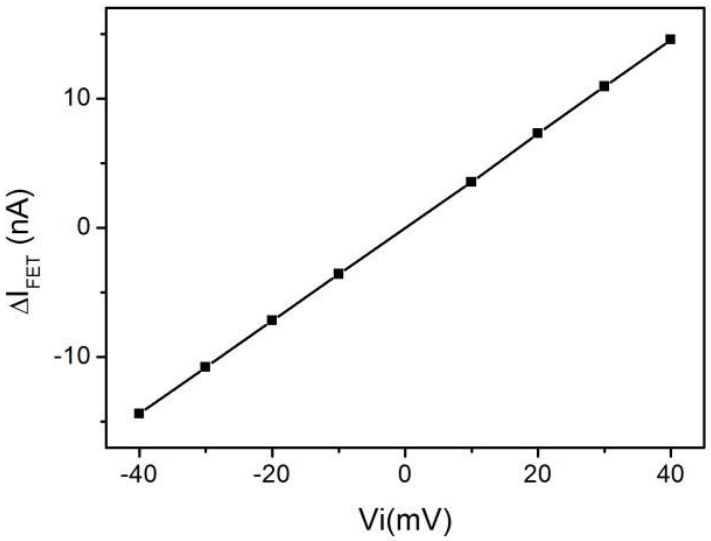

(b)

Figure 3-10 Effect of doping potential on (a) ΔI_{FET} (b) $\Delta I_{FET}/I_{FET}$.

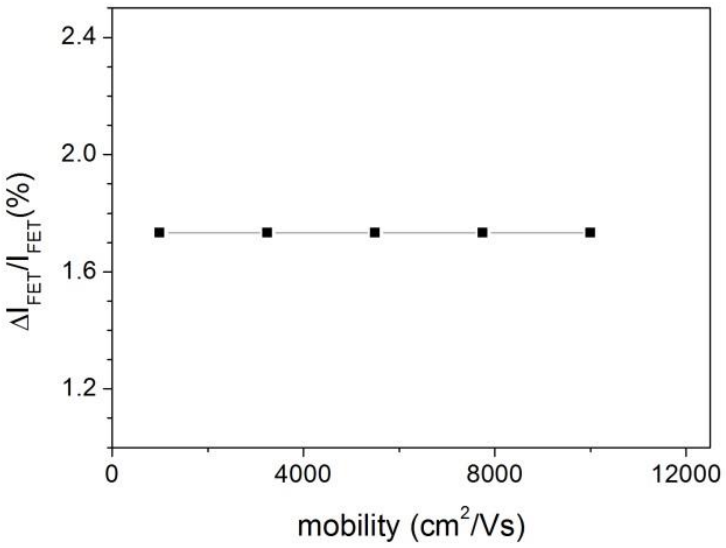

(a)

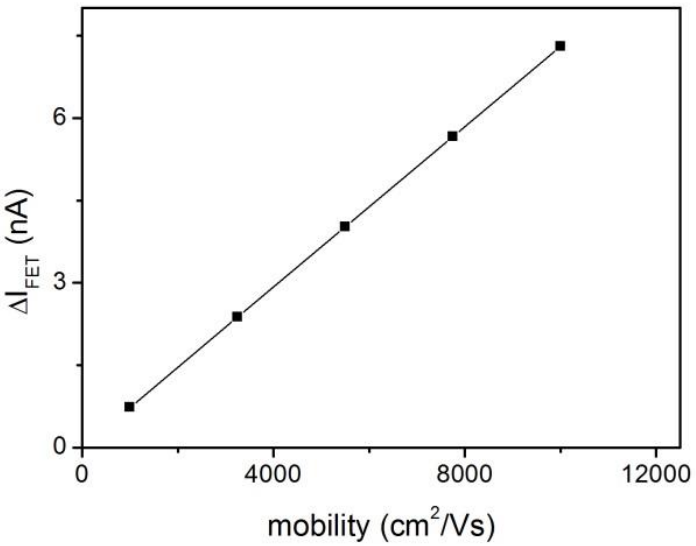

(b)

Figure 3-11 Effect of mobility on (a) ΔI_{FET} (b) $\Delta I_{FET}/I_{FET}$.

6. References

[1] F. Traversi, C. Railon, S. M. Benameur, K. Liu, S. Khlybov, M. Tosun, D. Krasnozhon, A. Kis, A. Radenovic, *Nature Nanotech.* **8**, 939 (2013)

[2] P. Xie, Q. Xiong, Y. Fang, Q. Qing, C. Lieber, *Nature Nanotech.* **7**, 119 (2012)

[3] M. Puster, J. A. Rodriguez-Manzo, A. Balan, M. Drindic, *ACS Nano*, published online (Nov. 13. 2013)

Chapter 4. Fabrication of graphene FET-nanopore

1. Overview

The overall device fabrication steps are illustrated in figure 4-1. Firstly, membrane is fabricated using photolithography and subsequent Reactive Ion Etching (RIE) of silicon nitride (SiN) layer and KOH etching of silicon. In the second step, metal electrode made is patterned using photolithography and subsequent lift off process. Then, large pore of diameter of 300nm is formed on SiN membrane using Focused Ion Beam (FIB). The next step is transfer of graphene grown on copper foil via Chemical Vapor Deposition (CVD) method onto the membrane and patterning of the graphene layer by photolithography and oxygen plasma etching. After that, thin aluminum oxide layer is deposited on the device surface using Atomic Layer Deposition (ALD). Finally, in the last step, pore with size of a few nanometer is drilled in TEM. In the following chapters, detailed processes of each step are described and issues associated with device fabrication are highlighted.

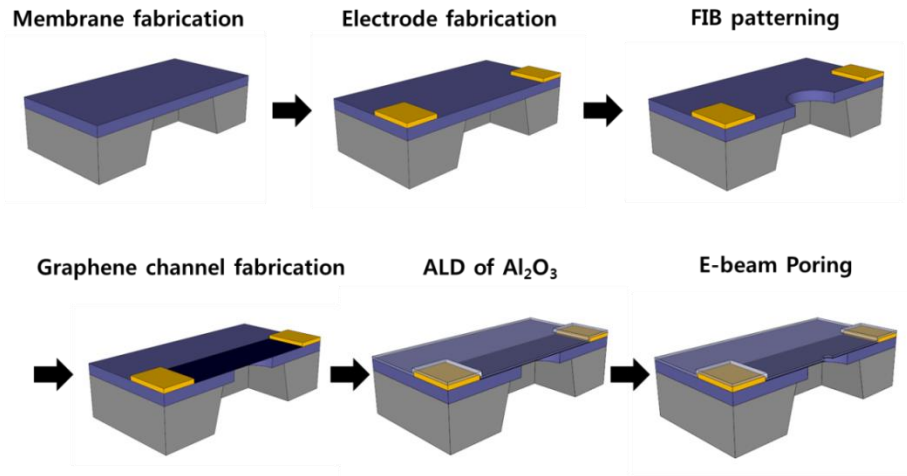

Figure 4-1 The overall fabrication steps.

2. Fabrication process

2.1 Membrane fabrication

Firstly, 100nm thick silicon nitride layer is deposited on double side polished Si wafer. Then, photolithography is used to define square of 750μm x 750μm. Following Reactive Ion Etching (RIE) in CF4 plasma results in 750μm x 750μm square opening of silicon nitride layer. Next anisotropic etching of silicon using KOH solution leads to formation of 50μm x 50μm square membrane region.

2.2 Electrode fabrication

Electrode is also fabricated using photolithography. Before starting electrode fabrication, membrane is cleaned in SPM solution (H_2SO_4:H_2O_2=4:1) to remove any organic contaminant. Then, Photoresist is firstly defined and 3nm/30nm of Ti/Au layer is deposited using e-beam evaporation. Finally, metal layer is lift off in acetone. Figure 4-2 summarizes membrane and electrode fabrication steps and SEM image of resulting device structure is shown in Figure 4-3.

2.3 FIB patterning

In this step, pore with diameter of 300nm is patterned using FIB. SEM images of the patterned pore structure is presented in Figure 4-4

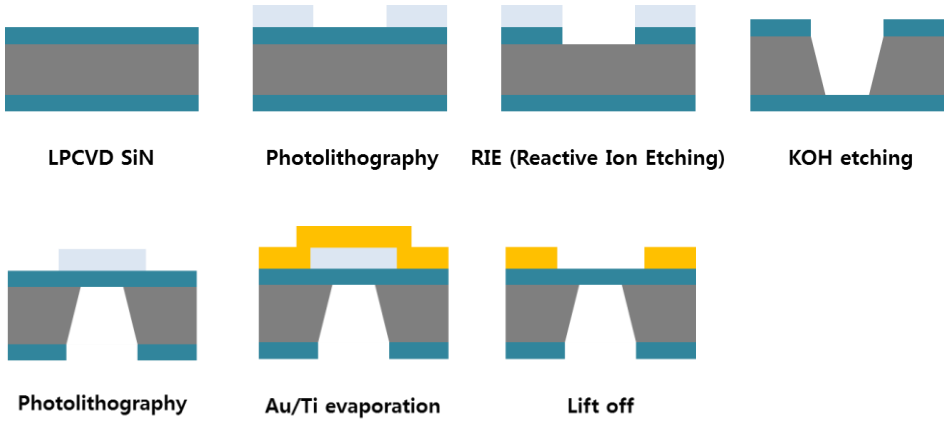

Figure 4-2 Membrane and electrode fabrication steps.

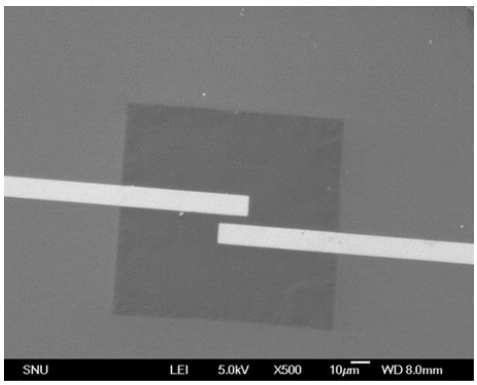

Figure 4-3 Low magnification SEM image of the device after electrode fabrication.

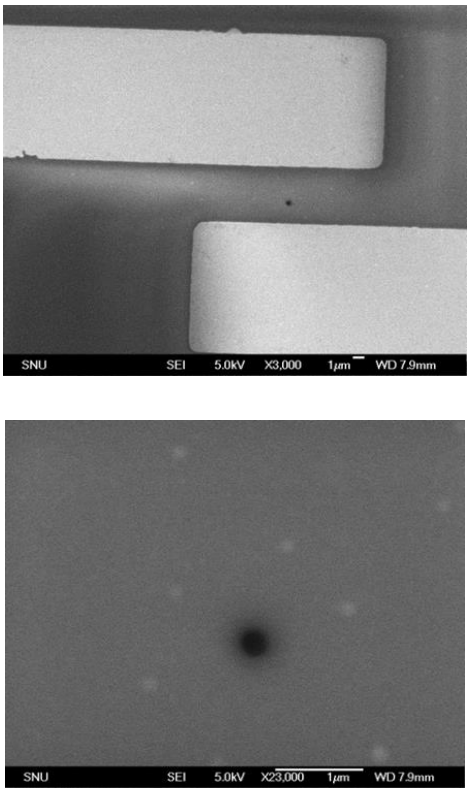

Figure 4-4 SEM images after FIB patterning.

2.4 Graphene channel fabrication

This step is quite delicate process. Firstly, single layer and full-coverage graphene is grown on copper foil in CVD chamber. [1] The preparation step for copper foil, growth temperature, gas flow rate should be optimally adjusted to produce high quality single layer graphene. Then, the graphene on copper foil is transferred onto the electrode patterned membrane using PMMA as a supporting layer. [2] The detailed procedure is illustrated in Figure 4-5. Graphene is spin coated with PMMA and soft baked. This PMMA/graphene/Cu foil layer is floated on Cu etchant to remove underlying Cu layer. After etching of Cu, PMMA/graphene layer is picked on substrate and washed several times to get rid of Cu etchant residues. Next, water remaining on the surface is dried at low temperature (~80℃) and the sample is further heated at 160℃ for 30min to ensure better adhesion between graphene and substrate. [3] Finally, PMMA on graphene is removed in acetone. Further rinse in ethanol and water is conducted to minimize PMMA residue on graphene.

The next step is patterning of graphene. This is done by photolithography. Firstly, photoresist is defined on graphene and evaporation deposition of Ni layer and lift off results in Ni mask pattern. Then, Graphene is etched in O_2 plasma condition. After the etching, Ni is removed in Ni etchant. Finally, graphene channel with length of 4μm and width of 6μm is fabricated. (see Figure 4-6.)

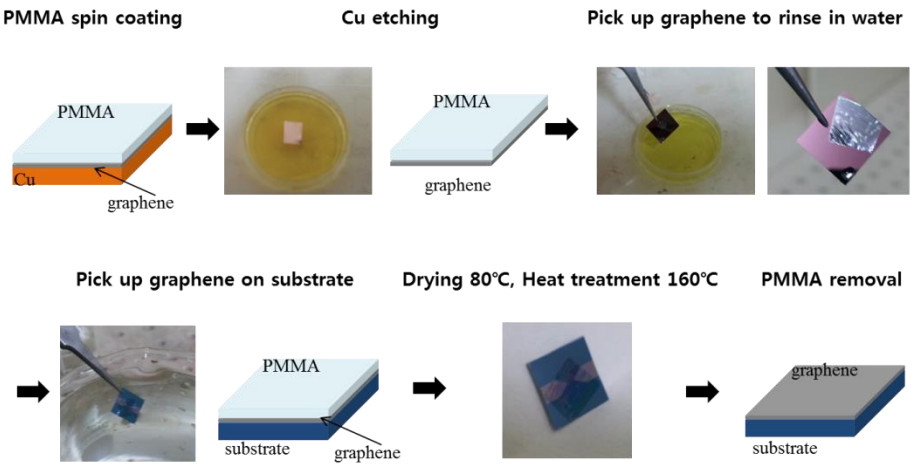

Figure 4-5 Graphene transfer process.

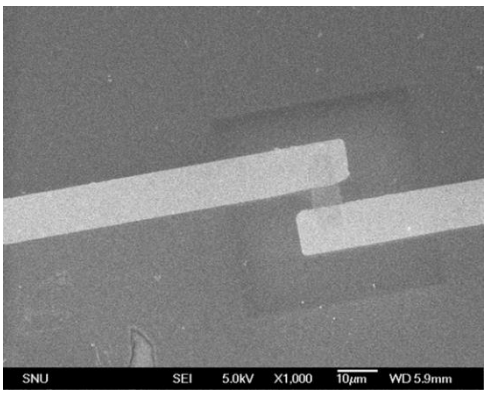

Figure 4-6 SEM image after graphene patterning.

After patterning the graphene, considerable amount of photoresist and PMMA residue exists on graphene. Therefore, cleaning of

graphene surface in vacuum chamber under Hydrogen atmosphere is required. [4], [5] The cleaning was conducted at 300℃ with H_2/Ar gas flow rate of 100sccm / 100sccm.

2.5 ALD of aluminum oxide layer

In order to deposition Al2O3 layer on graphene, firstly thin Al less than 2nm is evaporated on graphene. This Al layer is fast oxidized to form Al_2O_3 , which works as a seeding layer for subsequent ALD process. Then, 10nm thick Al_2O_3 layer is deposited using ALD.

2.6 E-beam poring

The last step is drilling nanopore using TEM. [6] Figure 4-7 shows one of the drilled nanopores.

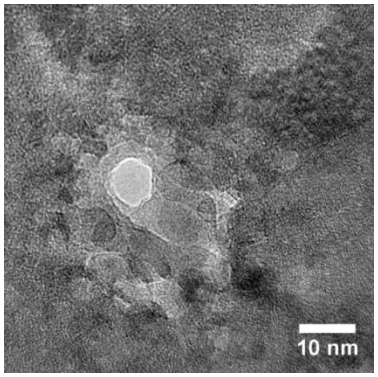

Figure 4-7 TEM image of nanopore.

3. Fabrication issues

The introduction of new material, graphene, requires quite amount of considerations on the device fabrication process design because graphene is not compatible with many conventional CMOS processes. In the followings, issues associated with graphene fabrication are discussed.

3.1 Mask material for graphene patterning

Graphene can be etched in oxygen plasma. The mask material for this oxygen plasma etching should satisfy several criteria. : (1) Of course, it must endure oxygen plasma. (2) it must be removable without damaging underlying graphene and leaving minimum residue. (3) It must show good adhesion with graphene.

Unfortunately, photoresist is influenced by oxygen plasma and it becomes hard to remove photoresist from graphene. Instead, graphene is torn away from the substrate because of stronger bonding between damaged photoresist and graphene. Therefore, search for new mask material other than photoresist is necessary for reliable patterning of graphene.

The next candidate for graphene patterning mask is Cu. Cu shows good resistance against oxygen plasma and can be easily removed in Cu etchant. Also, because Cu is catalyst material used for graphene growth, concern for residue is minimized. However, application of Cu as a mask material was not successful because of poor adhesion of Cu with graphene. During lift off of Cu, pattern that should remain on graphene was also washed away with acetone.

Finally, Ni is chosen for the mask material. Ni also has excellent resistance against oxygen plasma and can be easily removed in Cu etchant. Because cu etchant has been already used in transfer process, chemical residue except Ni is not of concern. Additionally, Ni shows better adhesion with graphene than that with Cu. For those reasons, Ni is appropriate for graphene patterning mask material. [7]

3.2 ALD on graphene

Deposition mechanism of ALD relies on surface reaction of precursor with surface groups or dangling bonds on the surface of substrate. However, graphene is 2D material absent from surface groups or dangling bonds except defect sites such as edges or cracks. Therefore, ALD of metal oxide on pristine graphene results in nonuniform deposition of oxide limited to defect sites. [8]

Several strategies have been developed to enable ALD on graphene. One method is to functionalize graphene to provide surface group using acid [8] or ozone treatment. [9] The other non-destructive method is to use thin seeding layer on graphene such as poly(4-vinylphenol) [10] or oxidized thin Al layer. [11] In my experiment, Al seeding layer method was utilized because of facileness of the process and nondestructive nature of the method.

3.3 Blockage of nanopore

After the formation of the graphene FET nanopore device, ionic conductance was measured and compared with calculated conductance value using the following equation.

$$G = e(n_K \mu_K + n_{Cl} \mu_{Cl}) \left(\frac{L_{pore}}{\frac{\pi}{4} {d_{pore}}^2} + \frac{1}{d_{pore}} \right)^{-1}$$

Where, e is unit charge of electron, n_K and n_{Cl} are the number of K^+ and Cl^- ions per unit volume, μ_K and μ_{Cl} are the mobilities of K^+ and Cl^-, L_{pore} is the length of a nanopore, and d_{pore} is the diameter of a nanopore. Comparison of experimentally measured ionic current with as a function of transmembrane voltage with calculated value is displayed in Figure 4-8. The measured ionic current is much smaller than the calculated one. The result suggests that pore diameter has been shrunk and blocked before the measurement. All of the samples after nanopore drilling showed the same result. : blockage of the nanopore.

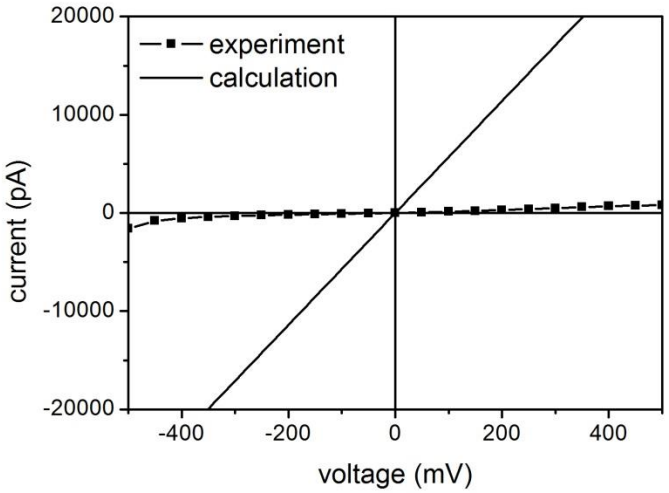

Figure 4-8 Measured and Calculated ionic current as a function of transmembrane voltage. Pore diameter of 10nm and pore length of 12nm were used for the calculation.

It has been reported that hydrocarbon can be a source of deposition of carbon on graphene while drilling of nanopore. [12] Possible candidates for hydrocarbon residue on graphene are PMMA from graphene transfer process or photoresist from graphene patterning process. In order to clarify the reason for pore blockage phenomena, 4 transferred graphene underwent the following four different processes, respectively. (1) No heat treatment (2) Annealing under H2 atmosphere at 200℃ (3) Annealing under H2 atmosphere at 300 (4) Annealing under H2 atmosphere at 400℃ after coating and removal of photoresist.

Then, nanopores were drilled to see effect of PMMA and photoresist residue on pore blockage. Firstly, effect of PMMA residue was studied by comparing samples (1), (2) and (3). The speed of pore blockage of sample (1) was faster than the speed of drilling of nanopore, making it impossible to form a nanopore. On the contrary, both the second and the third sample, which underwent hydrogen cleaning process were successfully drilled and no pore blockage was observed. Also TEM image showed that samples underwent 300℃ annealing is thinner than the samples underwent 200℃ annealing. With increasing annealing temperature, lesser PMMA residue is expected. [4], [5] Based on the experimental results, it can be concluded that although PMMA residue can lead to blockage of nanopore, PMMA can be effectively removed using hydrogen cleaning process and becomes not problematic anymore.

However the fourth sample with photoresist residue suffered from severe pore blockage speed even though it underwent hydrogen cleaning process. It seems that photoresist cannot be effectively removed by the cleaning step. Thus, major origin of the pore blockage

of the graphene FET nanopore is turned out to be the photoresist residue. In order to prevent this problem, PMMA instead of photoresist can be used as a E-beam resist to pattern graphene.

4. References

[1] X. Li, W. Cai, J. An, S. Kim, J. Nah, D. Yang, R. Piner, A. Velamakanni, I. Jung, E. Tutuc, S. K. Banerjee, L. Colombo, R. S. Ruoff, *Science* **32**, 1312 (2009)

[2] A. Reina, X. Jia, J. Ho, D. Nezich, H. Son, V. Bulovic, M. S. Dresselhaus, J. Kong, *Nano Lett.* **9**, 30 (2009)

[3] J. W. Suk, A. Kitt, C. W. Magnuson, Y. Hao, S. Ahmed, J. An, A. K. Swan, B. B. Goldbera, R. S. Ruoff, *ACS Nano* **5**, 6916 (2011)

[4] Z. Cheng, Q. Zhou, C. Wang, Q. Li, C. Wang, Y. Fang, *Nano Lett.* **11**, 767 (2011)

[5] Y. Lin, C. Lu, C. Yeh, C. Jin, K. Suenaga, P. Chiu, *Nano Lett.* **12**, 414 (2012)

[6] M. D. Fischbein, M. Drindic, *Appl. Phys. Lett.* **93**, 113107 (2008)

[7] S. Kumar, N. Peltekis, K. Lee, H. Kim, G. S. Duesberg, *Nanoscale Research Lett.* **6**, 390 (2011)

[8] X. Wang, S. M. Tabakman, H. Dai, *J. Am. Chem. Soc.* **130**, 8152 (2008)

[9] S. Jandhyala, G. Mordi, B. Lee, G. Lee, C. Floresca, P. Cha, J. Ahn, R. M. Wallace, Y. J. Chabal, M. J. Kim, L. Colombo, K. Cho, J. Kim, *ACS Nano* **6**, 2722 (2012)

[10] W. C. Shin, T. Y. Kim, O. Sul, B. J. Cho, *Appl. Phys. Lett.* **101**, 033507 (2012)

[11] S. Kim, J. Nah, I. Jo, D. Shahrjerdi, L. Colombo, *Appl. Phys. Lett.*

94, 062107 (2009)

[12] B. Song, G. F. Schneider, Q. Xu, G. Pandraud, C. Dekker, H. Zandbergen, *Nano Lett.* **11**, 2247 (2011)

Chapter 5. Summary and conclusion

A FET nanopore system can be used to detect DNA by monitoring FET current change during DNA translocation. Among many other nanopore platforms, this detection mechanism has advantages in large signal (~nA) enough to be detected and easier fabrication. In addition, the most important advantage is possibility of integration of the devices on single membrane, enabling high throughput DNA sequencing.

Previously developed silicon nanowire FET system is shown to be able to detect translocation of single DNA. However, this system suffered from limited working ion concentration range and quite low relative change of signal. In this thesis, graphene is introduced as a FET material to overcome such limitations of the silicon nanowire FET nanopore system. The key advantage of graphene is its transfer characteristic, dependence of drain current on gate voltage, enabling device to work at gate voltage close to zero. Also, there are additional advantages of using graphene including easiness of fabrication and fast device operation speed and stability in ionic solution.

A Numerical model was developed to anticipate operation of graphene FET nanopore device and manifest superiority of using graphene over silicon nanowire. The simulation result suggested that graphene FET can detect DNA even in 1M KCl solution, which were not possible for silicon nanowire FET device. Also, its relative signal change was much larger than that of silicon nanowire. In next step, this model was verified by comparing simulation result with experimental result. Although there was a little bit of difference in magnitude, presumably due to effect of surface charge, simulation results well described the experimental result. Lastly, the model was applied to find out the optimum device parameter to be utilized for the device design.

Based on the knowledge of the optimum device design, devices were fabricated. The device fabrication was quite challenging due to the presence of graphene. Fabrication issues and their solutions were summarized. The most critical problem was blockage of nanopore, originating from photoresist residue remaining after graphene patterning process. E-beam patterning of graphene using PMMA as a E-beam resist is suggested to prevent blockage of nanopore.

Further work to complete device fabrication and study effect of surface charge by varying pH and salt concentration can be a meaningful job.

Abstract (in Korean)

나노포어 구조는 다양한 방식으로 단일 분자 검지 및 DNA 염기 서열 분석에 활용될 수 있다. 본 연구에서는 나노포어 구조에 그래핀 트랜지스터를 결합하여 DNA의 통과를 좀 더 정밀하고 빠른 속도로 검지 할 수 있는 소자를 제안하고자 한다. 최근에 실리콘 나노와이어 트랜지스터를 이용하여 DNA가 지나갈 때 발생하는 포텐셜 변화를 감지하는 연구가 발표된 바 있다. 하지만 실리콘 나노와이어를 그래핀으로 대체할 경우 소자가 작동 가능한 이온 농도 조건에 제약을 받지 않게 되며 상대적인 전류 신호 변화도 커서 좀 더 정밀한 검지가 가능하다. 또한 그래핀의 높은 전하이동도 덕분에 소자가 빠른 속도로 작동 가능하며 화학 안정성이 이온 용액안에서 작동하는 소자의 내구성을 증가시킬 수 있다.

본 연구에서는 그래핀 트랜지스터 나노포어 소자를 시뮬레이션 할 수 있는 모델을 개발하였다. 이 모델을 이용하여 소자의 성능을 예측하고 기존의 실리콘 나노와이어를 이용한 소자와 비교할 수 있었다. 시뮬레이션과 실험 결과의 비교를 통하여 모델을 검증 할 수 있었다. 또한 나노포어의 길이, 나노포어의 지름, 그래핀 채널의 너비, 그래핀 채널의 길이, 그래핀 채널의 도핑 레벨, 그래핀의 전하 이동도 등의 변수들의 영향을 시뮬레이션 하고 해석함으로써 소자의 설계를 최적화 하고자 하였다. 다음으로 이를 바탕으로 기존의 top-down 공정을 이용하여 소자를 제작해 보았다. 그러나 그래핀이라는 새로운 물질을 도입함으로 인해 여러 문제들이 발생하였으며 이러한 문제들에 대해서 상세히 논해 보았다.

Acknowledgement (in Korean)

설레는 마음으로 연구실에 첫 출근하던 날이 엊그제 같은데 벌써 연구실을 떠나 새로운 출발점에 서게 되었습니다. 대학원에서 보낸 2년은 비록 짧은 시간이었지만 제게 무엇보다 값진 경험 이였습니다. 그 어느 때보다 저 자신과 앞으로의 삶에 대해 치열하게 방황하고 고민할 수 있었던 소중한 시간들이었던 것 같습니다. 그리고 그 동안 제가 성장할 수 있도록 옆에서 지켜봐 주시고 도와주신 주변 분들께 감사의 글을 전하고 싶습니다.

우선, 지도교수님인 김기범 교수님께 감사의 말씀을 드립니다. 대학원에 진학은 하였는데 막상 무엇을 어떻게 연구 해야 하는지 몰라 방황하던 저에게 무엇이든 네가 하고 싶은 일을 찾아보라며 다독여 주셨던 기억이 납니다. 교수님께서 Jimmy Xu 교수님과 함께 일 할 수 있는 기회를 만들어 주셨고 제가 스스로 새로운 연구 주제들을 들고 찾아갈 때면 언제나 열심히 들어주시고 같이 고민해 주셨습니다. 스스로 헤쳐나갈 수 있도록 옆에서 지켜봐 주시고 기회를 주셔서 감사합니다. 그리고 한동안 제 지도교수님이나 마찬가지이셨던 Jimmy Xu 교수님께도 감사 드립니다. Jimmy Xu 교수님과 함께 일할 수 있어서 영광이었고 연구에 있어서 작은 가능성도 놓치지 않는 자세를 배울 수 있었습니다. 또한 바쁘신 와중에도 제 졸업 심사 위원을 맡아주신 김미영 교수님과 남기태 교수님께도 감사의 말씀을 드립니다. 덕분에 저의 연구를 좀 더 객관적으로 바라 보고 부족한 점을 찾을 수 있었습니다.

그리고 가족처럼 동고동락한 나노공정연구실 구성원들께 감사의 말씀을 전하고 싶습니다. 제가 대학원 생활을 통해 얻은 가장 큰 자산은 실험실에서 만났던 선후배님들과의 인연이 아닌가 싶습니다.

우선 실험실의 최고참 선배님이신 현미 언니께서는 제가 연구에 첫 발을 내딛을 수 있도록 도와주셨습니다. 해박한 지식과 오랜 경험을 바탕으로 제가 연구 주제를 잡고, 실험들을 설계하고 해쳐나갈 수 있도록

도와주셔서 감사합니다. 그리고 어려운 일이 있을 때마다 아낌없이 조언해 주시고 격려해 주셔서 감사합니다.

항상 근면 성실한 모습으로 후배들에게 모범이 되셨던 도중 오빠, 부족한 저를 실험에 참여 시켜 주시고 논문 저자에도 포함 시켜 주셔서 감사합니다. 덕분에 석사 졸업 전에 제 이름이 들어가 있는 논문 한 편을 갖게 되어서 얼마나 기뻤는지 모릅니다. 브라운 대학교에서도 연구 잘 하시리라 믿습니다. 그리고 제 실험을 가장 많이 도와 주셨던 민현이 오빠, 반공연을 누비며 자유자재로 장비들을 다루던 모습이 대단해 보였던 기억이 납니다. 워낙 다재다능 하셔서 공정, 시뮬레이션, 측정 등 다양한 측면에서 제게 많은 도움을 주셔서 감사했습니다.

같은 AIPEL 팀이였던 승우 오빠와 민이 언니께도 감사를 드립니다. 승우 오빠와는 한 학기 밖에 같이 지내지 않았었지만 혼신의 fabrication 정신을 배울 수 있었습니다. 그리고 Jimmy Xu 교수님과 함께 일하면서 어려운 점이 있을 때마다 같이 고민해주시고 조언해 주신 민이 언니께도 감사 드립니다. 항상 긍정적이고 밝은 모습으로 생활하는 자세를 본받고 싶습니다.

궂은 일도 앞장서서 하고 책임감 있는 모습을 보여 주셨던 기용이 오빠, 용기 있는 결정을 하신 만큼 원하는 길을 잘 찾아가실 것이라고 믿습니다.

항상 유쾌한 농담으로 실험실 사람들을 즐겁게 해 주셨던 재일이 오빠, 낯을 가려 조용하던 저에게 먼저 다가와 말을 걸어주셔서 감사했습니다. 덕분에 실험실에 잘 적응하고 연구실 사람들과 잘 어울려 지낼 수 있었던 것 같습니다.

저를 많이 예뻐해 주셨던 승현이 오빠, 저에게 이것 저것 친절하게 알려주셔서 감사했습니다. 열심히 이 빔 리소그래피 장비까지 알려주셨는데 장비만 배우고 도망가서 죄송하네요. 올해에는 바라시던 데로 졸업 성취하시길 바랍니다.

처음에는 가장 다가가기 어려웠지만 지금은 가장 편해진 그래핀팀

선배님들 성용 오빠와 기주 오빠에게도 감사의 말씀을 드립니다. 졸업 준비하는 동안 일이 잘 풀리지 않을 때마다 두 분께 행패를 부리곤 했었는데 화내지 않고 참아 주셔서 감사합니다. 두분 덕분에 숨겨져 있던 저의 모습을 발견 할 수 있었던 것 같습니다. 항상 깔끔하고 야무지게 일처리를 하시던 성용이 오빠는 그래핀과 박막 증착에 대한 해박한 지식으로 제게 많은 도움을 주셨습니다. 저를 자주 괴롭히시긴 했지만 연구뿐만 아니라 여러 측면에서 제가 가장 의지를 많이 했던 선배인 것 같습니다. 저에게 장난을 많이 치셨던 기주 오빠는 저의 멍청한 실수들을 항상 적나라하게 지적해 주시며 저의 발전을 도와 주셨습니다. 또한 저를 환경 안전 부장에 임명해주신 덕분에 책임감 있게 일하는 법에 대해 배울 수 있었습니다. 요즘 방장 일 하시느라 바쁘신 것 같은데 도움이 못 되어서 죄송하네요.

나노 포어팀을 이끌고 계신 경범이 오빠는 여러모로 본 받을 점이 많은 것 같습니다. 많은 후배들을 거느린 부담스러운 자리임에도 불구하고 조용히 자기 할 일을 해나가는 모습이 존경스럽습니다. 여간 해서는 흔들리지 않는 강한 정신을 갖고 계신 것 같아 항상 부럽습니다. 그리고 나노 포어 분야에 대해 조언을 해 주시며 저의 졸업을 함께 걱정해 주셔서 감사합니다.

연구실 입학 동기인 정모 오빠와 형준 오빠 에게도 감사의 말씀을 드립니다. 동기들과 함께 하였기에 어렵고 힘든 일들도 잘 헤쳐나갈 수 있었던 것 같습니다. 제가 정모 오빠를 잘 못 된 수업에 끌어들인 바람에 같이 여러 밤을 지새우며 고생하였던 기억이 납니다. 디펜스 준비 때에도 정모 오빠와 함께였기 때문에 더 힘이 났던 것 같습니다. 멋쟁이 형준이 오빠는 제게 항상 다 잘 될 테니 너무 걱정하지 말라며 위로해 주셨던 기억이 납니다. 힘들고 귀찮은 일들을 함께 하였던 사람들이기에 더욱더 고마운 것 같습니다.

한 학기 늦게 들어오신 홍식이 오빠와 천광이 오빠께도 감사의 말씀을 드립니다. 설득 심리학의 달인이신 홍식이 오빠는 요즘 연구에 신이 나신 것 같아 보기 좋습니다. 지금처럼 계속 연구에 매진하신다면 좋은 결과가

있을 것이라 믿습니다. 가끔 허당 같은 모습을 보여주시며 연구실 사람들에게 즐거움을 주셔서 감사합니다. 옆자리 짝궁이신 천광이 오빠는 요즘 고생이 많으신 것 같지만 꿋꿋하게 이겨내시며 사회생활 선배님으로써 존경스러운 모습을 보여주고 계십니다.

다음으로 연구실에 활력을 불어 넣어준 다섯 후배님들께도 감사의 말씀을 드립니다. 처음으로 받는 후배들이었기에 어떤 사람들이 오게 될지 궁금했었는데 다들 똑똑하고 개성 넘치는 사람들이어서 좋았습니다. 뒤늦게 나노포어 연구를 시작하면서 사실 후배님들께 가르쳐 준 것 보다 배운 것이 더 많은 것 같아 항상 미안하고 고맙습니다. 민수 오빠는 제게 '짐선배'라는 별명을 붙여주시고 부족하고 나이도 어린 저를 선배처럼 생각해 줘서 감사했습니다. 아직 인정 받고 있지 못한 것 같지만 누구보다 연구에 열정적이시고 열심이시기 때문에 앞으로 좋은 결과가 있을 것이라 믿습니다. 그리고 재현이 오빠는 발군의 컴퓨터 실력으로 연구실의 컴퓨터 관련 업무들을 담당할 수 있을 것으로 기대하고 있습니다. 홈페이지 관리 업무도 흔쾌히 맡아주셔서 감사합니다. 학부 동기인 재석이는 제게 가장 힘이 많이 되었던 후배입니다. 저를 너무 좋게 봐 주어서 고마웠고 디펜스 준비로 힘들어 할 때 건네준 몇 마디 말들이 제게 큰 용기가 되었습니다.

동갑인 영호는 항상 자신감 넘치고 당당한 모습이 좋아보입니다. 저의 무식함을 꼬집어내는 능력으로 보아 그래핀 팀에 정말 적합한 친구라는 생각이 듭니다. 혼자 ALD를 맡고 있어 어려움이 있는 것 같지만 똑똑한 친구이니 잘 해내리라 믿습니다. 또 한 명의 동갑내기이자 연구실 막내인 기단이는 남자들 틈에서도 기죽지 않고 잘 어울리고 있는 것 같아 보기 좋습니다. 처음 나노포어 연구를 시작할 때 제게 아낌없이 멤브레인을 제공해주며 나노포어 실험과 관련하여 이것저것 물어보면 친절히 대답해 주어 고마웠습니다. 무엇보다도 충분히 저를 놀릴 수 있는 능력이 있음에도 불구하고 참아준 것이 대단히 고맙습니다.

연구실에 없어서는 안될 혜진이 언니와 정은이 언니께도 감사의 말씀을 드리고 싶습니다. 출산 때문에 혜진이 언니가 자리를 비웠던 짧은 기간 동안 혜진언니의 빈자리를 통감할 수 있었습니다. 그만큼 저희 연구실에

없어서는 안 될 중요한 역할을 하고 계십니다. 육아와 일을 병행하시며 힘드신 것 같지만 잘 해내시리라 믿습니다. 나노포어를 열심히 뚫어주셨던 정은이 언니께도 감사의 말씀을 드립니다. 잘 뚫리지도 않는 샘플을 눈이 빠져라 뚫어주시려고 노력해 주셔서 정말 감사합니다. 요즘 정은 언니는 결혼 준비로 바쁘신 것 같던데 결혼 준비 잘 하시고 예쁜 가정 꾸려나가시길 바랍니다.

마지막으로, 저를 지금 이 자리에 있게 물심양면으로 지원해준 가족께 감사의 말씀을 드립니다. 가족을 위해 쉬는 날도 없이 열심히 일하시는 아빠, 항상 제가 하고 싶은 일을 할 수 있도록 용기를 주시는 엄마, 늦은 밤 퇴근하는 누나를 항상 기다려주는 귀여운 동생 동희, 내색은 잘 안 하셨지만 누구보다도 서울대생인 손녀딸을 자랑스러워 하셨던 할머니 모두 제게 든든한 후원군이었습니다.

다시 한번 도움을 주신 모든 분들께 진심으로 감사하는 마음을 전하며 글을 마치겠습니다.

2014년 2월 김지연